JOC The Journal of Organic Chemistry

Article

Synthesis, Characterization and Properties of Diazapyrenes Via Bischler-Napieralski Reaction

Yi Han, Zhenzhu Hu, Meifang Liu, Mengwei Li, Tingting Wang, and Yulan Chen

J. Org. Chem., **Just Accepted Manuscript** • Publication Date (Web): 26 Feb 2019

ACS Publications

is published by the American Chemical Society. 1155 Sixteenth Street N.W., Washington, DC 20036

Synthesis, Characterization and Properties of Diazapyrenes Via Bischler-Napieralski Reaction

Yi Han,[†§] Zhenzhu Hu,[†§]Meifang Liu,[‡] Mengwei Li,[*†] Tingting Wang[†] and Yulan Chen[*†]

[†] Tianjin Key Laboratory of Molecular Optoelectronic Science, Department of Chemistry, Tianjin University, Tianjin, 300350, P. R. China.

[‡] Department of Chemistry, Weifang University, Weifang, 261061, P. R. China.

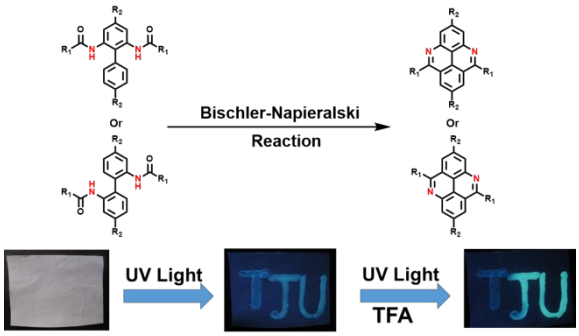

Abstract

Via Bischler-Napieralski cyclization of amide precursors as the key step, a series of diazapyrene derivatives were designed and successfully synthesized. Their crystal structures, optoelectronic properties and acid-responsive feature were investigated, which demonstrated that the doping of nitrogen atoms to the pyrene framework remarkably modulates their physical and chemical properties.

Keywords: diazapyrenes, Bischler-Napieralski cyclization, acid-responsive feature

1. Introduction

Polycyclic aromatic hydrocarbons (PAHs) are of considerable academic and industrial importance due to their excellent charge-transfer abilities,[1] and broad functionality with tunable optophysical properties.[2] Pyrene, as the simplest peri-fused PAH, is a typical fluorogenic motif and ideal building block for constructing large conjugated systems.[3] Pyrene chemists have greatly extended the variety of available protocols to synthesize various functionalized pyrenes for diverse applications.[4] Among these protocols, doping heteroatoms to the lattice of aromatics is an effective strategy to modulate their intrinsic physicochemical properties.[5] Concerning the potential dopants, electronegative nitrogen has a smaller atomic radius and one more electron than carbon.[6] Thus, chemical doping of nitrogen into pyrene is of interest for novel photophysical, electrochemical and responsive properties.[7]

4,10- and 4,9-azapyrenes are the nitrogen isosteres of pyrene with two nitrogen

atoms at different sites of pyrene skeleton (Scheme 1), which can be served as promising candidates for biomolecular probes, chemosensors and optoelectronic devices. However, literature precedents on 4,10-, 4,9-azapyrenes and their derivatives are limited, mainly because the synthetic procedures require multi-steps and harsh reaction conditions. As a result, systematic investigations of the optophysical properties of these aza-analogues have rarely been reported.[8] Moreover, to make diazapyrene-containing macromolecules or other functional materials, their corresponding dihalogenated derivatives should be synthesized first. Unfortunately, attempted halogenation of diazapyrene failed based on previously reported protocols.[9] Therefore, the development of efficient synthetic methods to achieve regioselective incorporation of nitrogen atoms into pyrene, for instance, to afford 4,10-, 4,9-azapyrenes and their dibromo-substituted derivatives, is highly desirable yet challenging.

We recently reported the application of Bischler-Napieralski cyclization as the key step to prepare phenanthridine, 1,10-phenanthroline derivatives and S, N-heteroarenes. Considering the electron rich feature of thiophene group, this reaction works well with S, N-heteroarenes.[10] In this article, we extend this reaction to pyrene based materials. Herein, a series of diazapyrene derivatives (**4,10-NPy-1**, **4,10-NPy-2**, **4,9-NPy-1**, **4,9-NPy-Br**, Fig. 1) were designed and synthesized through Bischler-Napieralski cyclization of the corresponding amide precursors. We demonstrated that if the precursors were delicately designed with amide groups located at the "2-, 6-" or "2-, 7-" positions of biphenyl, two-folded

Bischler-Napieralski cyclization would facilely lead to the formation of diazapyrene cores with the N-doping at specific positions of the pyrene ring. We not only developed an efficient synthetic strategy to enrich the chemical diversity of diazapyrene compounds, but also studied the intriguing photophysical properties and acid-responsive behaviors of these compounds. Since pyrene chemistry is strongly position-dependent, our current efforts regarding various diazapyrene isomers greatly contribute to the understanding of fundamental structure-property relationship of diazapyrenes.

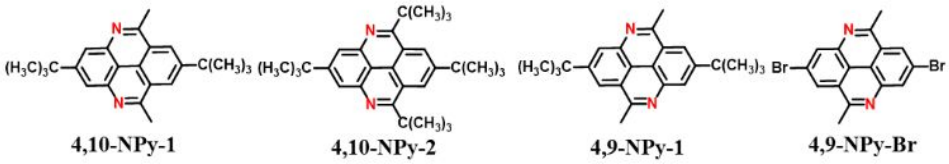

Fig. 1 Chemical structures of diazapyrene derivatives in this work.

2. Results and discussion

The structures and synthetic routes of the target compounds including substituted diazapyrenes with nitrogens at different sites (**4,10-NPy-1, 4,10-NPy-2, 4,9-NPy-1**), dibrominated diazapyrene (**4,9-NPy-Br**) and diazapyrene-based π-conjugated oligomer (**Fl-NPy**) are outlined in Scheme 1. First, 4-*tert*-butyl-2,6-dinitrobromobenzene ($\mathbf{N_1}$) was prepared by nitration of commercially available 4-*tert*-butylbromobenzene in a yield of 53%. Then, Suzuki-Miyaura cross-coupling reaction between $\mathbf{N_1}$ and *p*-*tert*-butyl benzyl boric acid was readily carried out by using $Pd(PPh_3)_4$ as the catalyst precursor, affording 2,6-dinitro-4,4'-di-*tert*-butylbiphenyl ($\mathbf{C_1}$) in a yield of 77%. Next,

2,6-diamino-4,4-di-*tert*-butylbiphenyl (**R_1**) was prepared from **C_1** with Fe powder as reductant, and **A_1-1** (or **A_1-2**) was obtained by the followed amidation with pivaloyl chloride (or acetyl chloride) in a total yield of 59% (or 60%) with the two steps. Finally, Bischler-Napieralski cyclization of these amides, using $POCl_3$ as the solvent and P_2O_5 as the catalyst under refluxing was accomplished successfully, with the target compounds (**4,10-NPy-1** and **4,10-NPy-2**) prepared in moderate yield (41% and 43%).

We also found that the Bischler-Napieralski cyclization herein was very sensitive to the substitution of the amides. For instance, **4,9-NPy-1** can be obtained under a synthetic route similar to **4,10-NPy-1**, but modified cyclization conditions are required, using ionic liquid of molten aluminum chloride–sodium chloride as the catalyst.[8] Moreover, as shown in Scheme 1, under similar reaction conditions, the intermediate **A_2-2** cannot be converted to the target compound **4,9-NPy-2**. This outcome is reasonable since the transformation of amide to 4,9-diazapyrene presumably involves two successive ring closures: carbonium-ion formation being followed by intramolecular electrophilic attack, which is greatly influenced by steric effect.[8,11] According to the optimal configuration of the amides (Fig. S1, Supporting Information), *tert-butyl* group existed in **A_2-2** has a larger steric hindrance than *methyl* in **A_2-1**, which may be not conducive to the electrophilic cyclization. In addition, to obtain functionable or polymerisable diazapyrene monomer, the dibrominated compound **4,9-NPy-Br** was successfully synthesized from the dibrominated amide precursor, which was not available by other reported approaches. As expected,

4,9-NPy-Br was demonstrated as a new building block for constructing new conjugated materials, for instance, by Suzuki coupling with 9,9-dioctyl-2-boronic ester-fluorene to afford **Fl-NPy** with a yield of 74%. *Tert-butyl* group existed in **A_2-2** has a larger steric hindrance than *methyl* in **A_2-1**.

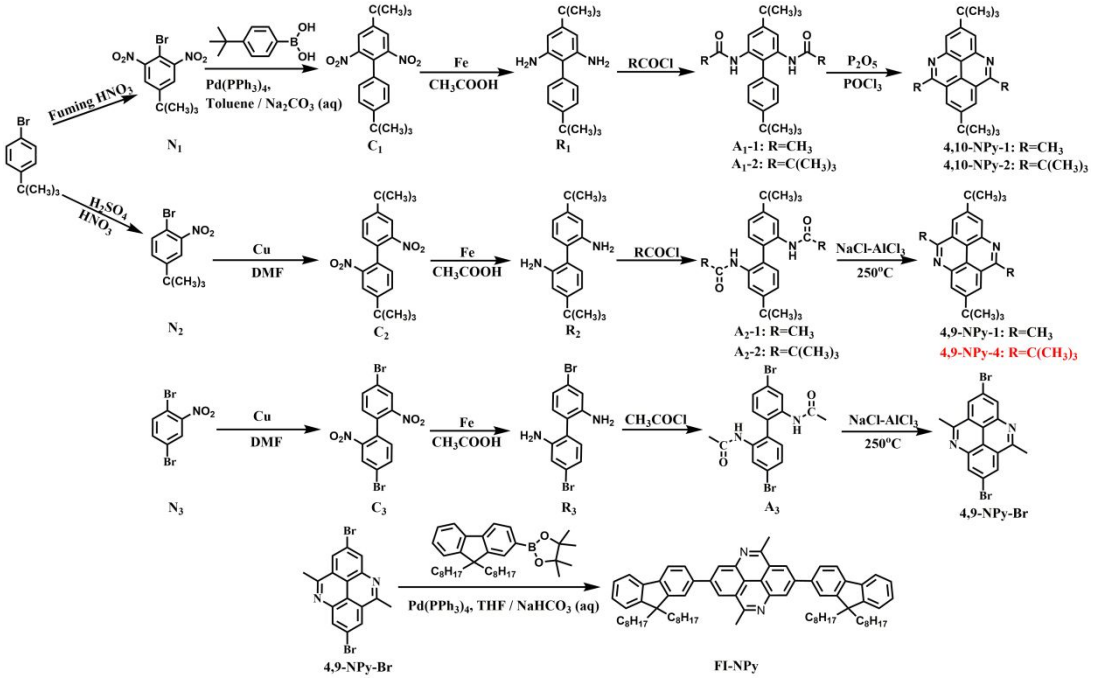

Scheme 1. Synthetic routes to **4,10-NPy-1**, **4,10-NPy-2**, **4,9-NPy-1, 4,9-NPy-Br** and **Fl-NPy**.

All target molecules can be dissolved in common organic solvents, such as dichloromethane, chloroform, and tetrahydrofuran, and were characterized by ^{1}H NMR and ^{13}C{1H} NMR spectroscopy as well as high-resolution mass spectrometry. The thermal properties of **4,10-NPy-1**, **4,10-NPy-2** and **4,9-NPy-1** were measured by the thermogravimetric analysis (TGA) under a nitrogen atmosphere. As shown in Fig. S5 (Supporting Information), they all exhibit good thermal stability with a weight loss of 5% at approximately 240 °C, indicating their high potential to be robust organic

materials.

Single crystals of **4,9-NPy-Br** suitable for X-ray measurements were obtained by slow evaporation of chloroform solutions in isopropyl alcohol atmosphere. The structure of **4,9-NPy-Br** was solved and refined in a triclinic *P*-1 space group. As depicted in Fig. 2, the main scaffold of **4,9-NPy-Br** showed small dihedral angles of less than 2°, consisting with the highly planar conformation of pyrene.[6] **4,9-NPy-Br** is arranged parallel to the dislocation packing motif driven by multiple intermolecular interactions, such as C-H···N and C-H···π interactions, with distances in the range of 2.59-2.89 Å. The shortest distance between the rigid planes consisted of the parallel neighboring molecules is 3.39 Å, manifesting the significant π-π interactions mainly stemmed from its large conjugation. Unfortunately, other crystals suitable for single-crystal X-ray diffraction were unavailable.

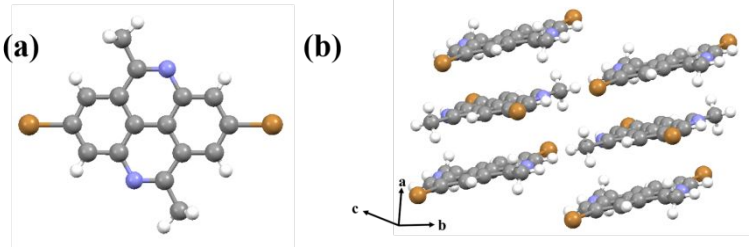

Fig. 2 (a) Single crystal structure and (b) packing diagram of **4,9-NPy-Br**.

Detailed photophysical properties of these diazapyrene molecules were investigated by UV-vis absorption and fluorescence spectroscopies. 2,7-Di-*tert*-butylpyrene **(Py-tBu)** was chosen as the reference compound to study the effect of nitrogen doping of pyrene on their optical properties.[12] It was found that in CH_2Cl_2 solution, all the four compounds exhibited well-resolved absorption bands in the range of 250-350

nm, which was attributed to the π-π* transition (Fig 3a). The distinct vibrational structures according to their absorption spectra, together with small Stokes shift of ca. 15 nm, revealed the rigidity of the skeleton. Compared to **Py-tBu**, the incorporation of nitrogen-atoms in **4,10-NPy-1**, **4,10-NPy-2** and **4,9-NPy-1** led to the additional n-π* transition with the appearance of absorption peaks at lower energy region at 360 and 380 nm.[13] Accordingly, narrower optical gaps of **4,10-NPy-1**, **4,10-NPy-2** and **4,9-NPy-1** were estimated from the onset of UV-vis absorption spectra as 3.19, 3.20 and 3.21 eV, respectively (E_g = 3.51 eV for **Py-tBu**), suggesting that the incorporation of nitrogen-atoms could reduce the energy gap of diazapyrenes.

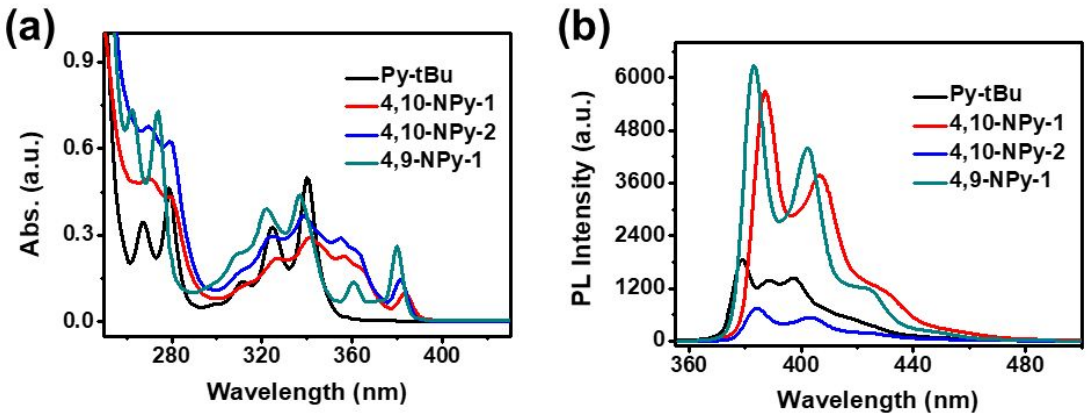

Fig. 3 (a) UV-vis absorption and (b) fluorescence spectra of **Py-tBu**, **4,10-NPy-1**, **4,10-NPy-2** and **4,9-NPy-1** (λ_{ex} = 340 nm) in CH_2Cl_2 (3.0 x 10^{-5} M).

All the four compounds showed blue emission in diluted solutions with emission peaks at about 380-400 nm (Fig. 3b). There was a large difference concerning their fluorescence quantum yields (Φ) (Table S3, Supporting Information). In detail, the fluorescence quantum yields of **4,10-NPy-1** and **4,9-NPy-1** in dilute CH_2Cl_2 solution were 25% and 26%, which were higher than that of **Py-tBu** (9%). As for **4,10-NPy-2**,

the value of Φ decreased remarkably (Φ = 2%), most probably because the stretching vibration of *tert*-butyl groups at the 5- and 9- positions promoted non-radiative dissipation of excited state.[14] Additionally, from solution to film, then solid state, the absorption for the three molecules exhibited red-shifting due to the increased aggregation effect (Fig. S7-9, Supporting Information).

Since the incorporation of heteroatoms into PAHs usually alters their electronic properties considerably, the electrochemical properties of these diazapyrenes and **Py-tBu** were then compared by using cyclic voltammetry (CV). Fig. 4 depicted a reversible oxidation wave for **Py-tBu** while irreversible and anodically shifted oxidation peaks for diazapyrenes in CH_2Cl_2. Accordingly, the HOMO energy levels of **Py-tBu**, **4,10-NPy-1**, **4,10-NPy-2** and **4,9-NPy-1** were estimated to be -5.59, -5.80, -5.89 and -5.81 eV, respectively, from the onset reduction potential with reference to Fc^+/Fc. The LUMO energy levels were calculated based on the absorption edges, which were -2.08, -2.61, -2.69 and -2.60 eV, respectively. The low-lying HOMO and LUMO energy levels of diazapyrenes manifested their potential application as p-type semiconductors.[15] All the photophysical and electronic data are summarized in Table S2.

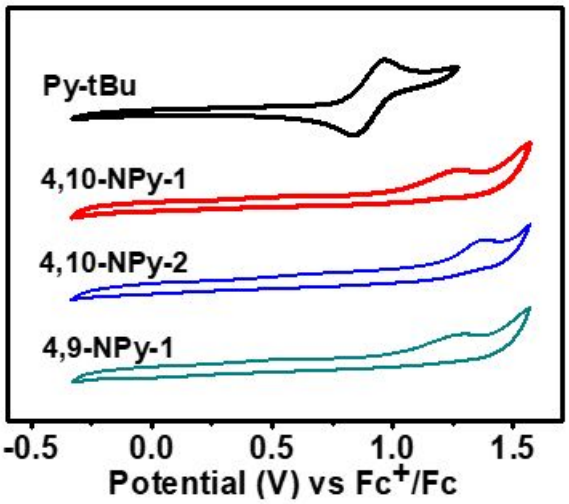

Fig. 4 Cyclic voltammograms of **Py-tBu, 4,10-NPy-1, 4,10-NPy-2** and **4,9-NPy-1** measured in CH_2Cl_2 with 0.1 M $TBAPF_6$ as electrolyte (scan rate = 100 mVs^{-1}).

To gain further insight into their electronic structures, the electronic distribution of HOMO and LUMO energy levels of these diazapyrenes were calculated by using Gaussian 09 software at the level of B3LYP/6-31G*. As shown in Fig. 5, their optimized structures displayed fully planar skeletons with electron density of the HOMO and LUMO delocalized over the whole molecules, indicating that there was no obvious intramolecular charge transfer (ICT) effect. With high electronegative nitrogen atoms in the pyrene framework,[7,16] all the molecules owned lower HOMO and LUMO levels compared to those of **Py-tBu**, which was also in good agreement with the experimental results.

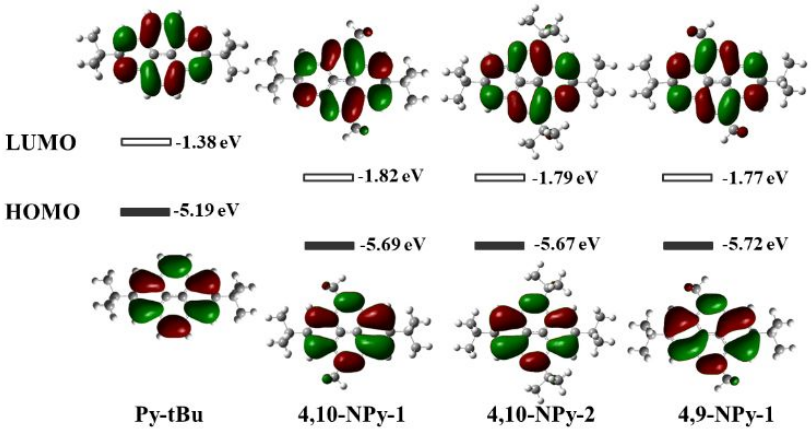

Fig. 5 Molecular-orbital amplitude plots and energy levels of the HOMOs and LUMOs for **Py-tBu**, **4,10-NPy-1**, **4,10-NPy-2** and **4,9-NPy-1** in the gas phase, as calculated at the level of B3LYP/6-31G*.

Furthermore, nitrogen-doped PAHs usually achieve their application as acid-responsive materials owing to the protonated ability of the nitrogen atom.[7,10a] In order to investigate the potential of these diazapyrenes to serve as acid-responsive materials, their protonation experiments in CH_2Cl_2 were carried out (Fig. 6, S10-12, Supporting Information). Taking **4,10-NPy-2** for example, with the addition of TFA from 0 to 50 eq, the absorption peaks at higher energy region from 306 to 365 nm decreased, accompanied by the appearance of long wavelength absorption band at 400 nm. The new absorption band implied the appearance of protonated species and could be attributed to the enhanced charge transfer transition.[17] Under 365 nm UV irradiation, the corresponding fluorescence spectra showed pronounced variation: the fluorescence intensity of **4,10-NPy-2** at 386 and 407 nm (purple-blue emission band) decreased dramatically, while a new bright blue-green emission peaked at 470 nm appeared and its intensity increased with the increase of TFA. The purple-blue

fluorescence of **4,10-NPy-2** can be recovered after treated with TEA, making it suitable for a turn-on sensor of H^+ (Fig. S11b, Supporting Information).

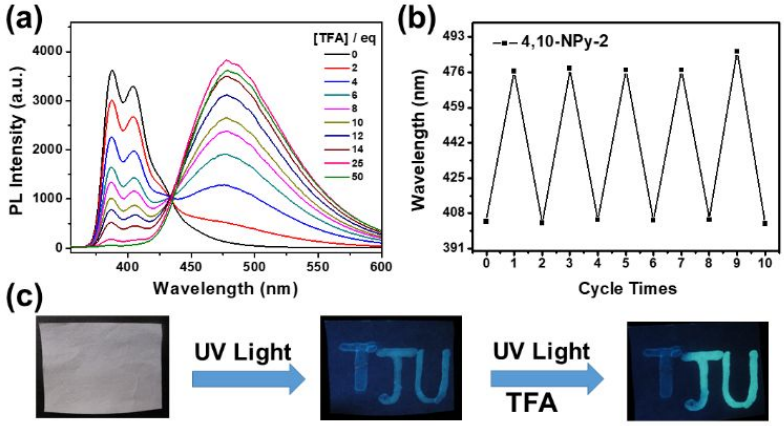

Fig. 6 (a) Fluorescence spectra of **4,10-NPy-2** in CH_2Cl_2 with different concentrations of TFA. (b) Switching the maximum emission wavelength of **4,10-NPy-2** sensor as a function of the fuming-air cycle numbers (λ_{ex} = 340 nm). (c) Photographs of **4,10-NPy-2** deposited on a piece of filter paper under daylight, before and after fumed with TFA vapor under UV light (The letter "T" was written with **Py-tBu** solution, and "J" and "U" were written with **4,10-NPy-2** solution).

Considering the unique acid responsive feature of these diazapyrenes in solution, their applications in solid-state fluorescent sensing devices were explored. Interestingly, it was found that all these materials can be utilized as security ink in a solid-state sensory system. One example is illustrated in Fig. 6c. Three letters (TJU) were written with **Py-tBu** (for the letter "T") and **4,10-NPy-2** (for the letters "J" and "U") solutions on the filter paper. At first, it was difficult to detect the presence of "TJU" by the naked eyes under daylight and when the filter paper was excited under a 365 nm UV lamp, the pattern presented as purple-blue "TJU". After being fumed with

TFA vapor, the letters "J" and "U" turned to light blue-green emission under UV irradiation while the letter written by **Py-tBu** was not responsive. Furthermore, this process is reversible and the blue pattern made from these diazapyrenes could be recovered when the paper was fumed with TEA vapor (Fig. S13-15, Supporting Information). This reversible process at room temperature makes diazapyrene a promising candidate for double security protection material.

3. Conclusions

Bischler-Napieralski cyclization of delicately designed amide precursors was demonstrated as a facile approach to synthesize a series of diazapyrene derivatives, which were found as smart materials with the ability to respond to acid both in solution and solid states. Using this strategy, not only the position of nitrogen atoms can be controlled, but also different substituted groups can be attached onto the pyrene ring, greatly facilitating the modulation of their optoelectronic properties and molecular geometries at the molecular level. Notably, the dibrominated diazapyrene synthesized by this method is a promising compound to develop various diazapyrene-based π-conjugated polymers or other macromolecular systems for diverse applications, and further investigations are in progress.

4. Experimental Section

General. Unless otherwise noted, the commercially available reagents were purchased from commercial suppliers and used without further purification.

Dichloromethane (CH_2Cl_2) was distilled over CaH_2. Tetrahydrofuran (THF) was purified by distillation from benzophenone and sodium. All reactions were monitored by TLC with silica gel 60 F254. Column chromatography was carried out on silica gel (200-300 mesh). The catalyst precursor $Pd(PPh_3)_4$ was prepared according to the literature [18], and stored in a Schlenk tube under nitrogen atmosphere.

Measurements. ^1H NMR (400 MHz) and $^{13}C\{1H\}$ NMR (100 MHz) spectra were recorded in deuterated solvents on a 400 MHz Bruker AV400 spectrometer. The high resolution electrospray mass spectra (ESI-TOF) of products were recorded on a micrOTOF-Q II 10204 mass spectrometer. FT-IR spectra of samples were recorded on a Bruker Model Alpha. Melting points were measured with SGW X-4A apparatus. Elemental analyses were recorded on Flash EA 1112. The UV-vis absorption spectra were obtained on PerkinElmer Lambda 750 spectrophotometer. Fluorescence spectra were recorded on a Hitachi F-7000 fluorescence spectrophotometer. Thermogravimetric analyses (TGA) were carried out using a TA Instruments Q-50 with a heating rate of 10 °C/min. Cyclic voltammetric experiments were carried out using a CHI 150E electrochemical workstation (CH Instruments, ChenHua, Shanghai, China). All voltammograms were acquired at room temperature. A standard three electrode electrochemical cell arrangement was employed using Pt carbon as working electrode, a Pt wire as counter electrode, and saturated calomel as reference electrode in 0.1 M tetrahydrofuran containing tetrabutylammonium hexafluorophosphate ($TBAPF_6$) as the supporting electrolyte with a sweep rate of 100 mVs^{-1}. The potentials are reported vs the Fc^+/Fc redox couple as a standard.

Synthesis

4-*Tert*-butyl-2,6-dinitrobromobenzene (N_1).[19] 4-*tert*-butylbromobenzene (20.00 g, 94.33 mmol) was added dropwise to stirred fuming nitric acid (50 mL) at 0 °C in an ice water bath. The mixture was stirred at 25 °C for 2h and then poured into vigorously stirring ice–water (200 mL). The yellow-green precipitate was collected by filtration and washed with water and saturated aqueous $NaHCO_3$ solution, affording the product as pale yellow-green needles (15.20 g, 53%). ^{1}H NMR (400 MHz, $CDCl_3$): δ 7.88 (s, 2H), 1.39 (s, 9H); $^{13}C\{^1H\}$ NMR (100 MHz, $CDCl_3$): δ 154.5, 151.7, 124.8, 103.9, 35.6, 30.7.

2,6-Dinitro-4,4'-di-*tert*-butylbiphenyl (C_1). A mixture of N_1 (3.00 g, 9.93 mmol), (*tert*-butyl) phenyl) boronic acid (2.60 g, 14.60 mmol), Na_2CO_3 (2.40 g, 22.64 mmol), TBAB (0.30 g, 0.93 mmol), toluene (50 mL) and H_2O (11 mL) was carefully degassed before and after $Pd(PPh_3)_4$ (0.30 g, 0.26 mmol) was added. The mixture was heated to reflux and stirred under nitrogen overnight. The reaction mixture was extracted with CH_2Cl_2 and washed with saturated brine. The combined organic layers were dried over anhydrous $MgSO_4$ and concentrated under reduced pressure. The residue was purified by chromatography on silica gel column eluting with petroleum ether/CH_2Cl_2 (v/v, 4/1) to afford C_1 as an ivory solid (2.80 g, 77%). ^{1}H NMR ($CDCl_3$, 400 MHz): δ 7.93 (s, 2H), 7.41 (d, J = 7.7 Hz, 2H), 7.16 (d, J = 7.6 Hz, 2H), 1.43 (s, 9H),1.33 (s, 9H).$^{13}C\{^1H\}$ NMR ($CDCl_3$, 100 MHz): δ 153.8, 152.3, 150.9, 127.8, 127.4, 127.1, 125.7, 123.5, 35.5, 34.7, 31.2, 30.8.

2,6-Diamino-4,4'-di-*tert*-butylbiphenyl (R_1). The mixture of glacial acetic acid (120

mL), C_1 (5.00 g, 13.58 mmol) and iron powder (11.00 g, 196.43 mmol) was heated at 80 °C for an hour. After cooling to room temperature, the iron powder was removed by filtration. After a large amount of water was added to the filtrate, solid appeared in the solution. The crude product was collected by filtration and used directly in the next step without further purification. The amidation yield is the total yield of two steps.

N,N'-(4,4'-Di-*tert*-butyl-[1,1'-biphenyl]-2,6-diyl)diacetamide (A_1-1). Acetyl chloride (5.00 g, 63.69 mmol) was added dropwise to the mixture solution of $\mathbf{R_1}$ (3.80 g, 12.83 mmol), triethylamine (5 mL) and anhydrous CH_2Cl_2 (120 mL) at 0 °C. After stirring at room temperature overnight, the reaction was quenched with water and extracted with CH_2Cl_2. The combined organic extracts were dried over anhydrous $MgSO_4$ and concentrated under reduced pressure. The residue was purified by chromatography on silica gel column eluting with CH_2Cl_2/EA (v/v, 5/1) to afford $\mathbf{A_1}$**-1** as a white solid (2.90 g, 59%). FT-IR (powder, cm^{-1}): 3318, 3198, 2957, 1664, 1515, 1420, 1358, 1267, 870, 833. mp 221–222 °C. ^{1}H NMR ($CDCl_3$, 400 MHz): δ 8.13 (s, 2H), 7.57 (d, J = 7.7 Hz, 2H), 7.21 (d, J = 7.3 Hz, 2H), 6.70 (s, 2H), 1.93 (s, 6H), 1.38 (d, J = 8.0 Hz, 18H). ^{13}C{^{1}H} NMR ($CDCl_3$, 100 MHz): δ 168.1, 152.2, 135.3, 130.1, 129.9, 126.9, 119.8, 114.9, 35.2, 34.9, 31.3, 31.2, 24.7. HRMS (ESI-TOF) m/z: $[M + Na]^+$ Calcd for $C_{24}H_{32}N_2NaO_2$ 403.2356; Found 403.2355. Anal. Calcd for $C_{24}H_{32}N_2O_2$: C, 75.75; H, 8.48; N, 7.36. Found: C, 75.81; H, 8.45; N, 7.52.

2,7-Di-*tert*-butyl-5,9-dimethylpyrido[5,4,3,2-lmn]phenanthridine (4,10-NPy-1). A solution of $\mathbf{A_1}$**-1** (0.30 g, 0.78 mmol), P_2O_5 (0.51 g, 3.59 mmol) and $POCl_3$ (8 mL)

was stirred at reflux for 24 h under N_2. After cooling to room temperature, water was added carefully to the solution. The aqueous phase was adjusted to pH = 9 with NaOH solution and extracted with dichloromethane, then dried over anhydrous $MgSO_4$ and evaporated to dryness. The product was purified by chromatography on alkaline Al_2O_3 column eluting with CH_2Cl_2 and the residue was recrystallized in methanol to afford **4,10-NPy-1** as a white solid (0.11 g, 41%). FT-IR (powder, cm^{-1}): 2953, 1591, 1476, 1365, 1269, 868, 728, 649, 559. mp 209–210 °C. ^1H NMR ($CDCl_3$, 400 MHz): δ 8.66 (s, 2H), 8.43 (s, 2H), 3.22 (s, 6H), 1.63 (s, 9H), 1.59 (s, 9H). $^{13}C\{^1H\}$ NMR ($CDCl_3$, 100 MHz): δ 159.4, 153.2, 150.0, 141.5, 125.6, 124.3, 124.1, 122.3, 110.6, 35.9, 35.8, 32.0, 31.9, 23.2. HRMS (ESI-TOF) m/z: $[M + H]^+$ Calcd for $C_{24}H_{29}N_2$ 345.2325; Found 345.2316. Anal. Calcd for $C_{24}H_{28}N_2$: C, 83.68; H, 8.19; N, 8.13. Found: C, 83.25; H, 8.45; N, 7.82.

N,N'-(4,4'-Di-*tert*-butyl-[1,1'-biphenyl]-2,6-diyl)bis(2,2-dimethylpropanamide) (A_1-2). **A_1-2** was synthesized following the procedure for **A_1-1,** with **R_1** (3.60 g, 12.15 mmol), Et_3N (5 mL), pivaloyl chloride (7.20 g, 59.71 mmol) in DCM (50 mL) as reagents. The desired product **A_1-2** was obtained as a white solid (3.80 g, 60%). FT-IR (powder, cm^{-1}): 3402, 3292, 2961, 1687, 1645, 1497, 1416, 1166, 1000, 863, 848, 665, 562. mp > 300 °C. ^1H NMR ($CDCl_3$, 400 MHz): δ 8.23 (s, 2H), 7.61 (d, J = 7.8 Hz, 2H), 7.23 (d, J = 8.0 Hz, 2H), 7.07 (s, 2H), 1.38 (s, 18H), 0.99 (s, 18H). $^{13}C\{^1H\}$ NMR ($CDCl_3$, 100 MHz): δ 176.1, 152.8, 135.6, 130.2, 130.1, 127.0, 119.2, 113.3, 39.7, 35.3, 34.9, 31.3, 27.2. HRMS (ESI-TOF) m/z: $[M + Na]^+$ Calcd for $C_{30}H_{44}N_2NaO_2$ 487.3295; Found 487.3294. Anal. Calcd for $C_{30}H_{44}N_2O_2$: C, 77.54; H,

9.54; N, 6.03. Found: C, 77.52; H, 9.71; N, 6.27.

2,5,7,9-Tetra-*tert*-butylpyrido[5,4,3,2-lmn]phenanthridine (4,10-NPy-2). **4,10-NPy-2** was synthesized following the procedure for **4,10-NPy-1**, with $\mathbf{A_1}$**-2** (0.50 g, 1.08 mmol), P_2O_5 (3.20 g, 22.54 mmol), and $POCl_3$ (15 mL) as reagents. **4,10-NPy-2** was obtained as a white solid (0.20 g, 43%). FT-IR (powder, cm^{-1}): 2972, 1619, 1557, 1467, 1364, 1196, 1158, 880. mp > 300 °C. ^1H NMR ($CDCl_3$, 400 MHz): δ 9.06 (s, 2H), 8.40 (s, 2H), 1.84 (s, 18H), 1.63-1.60 (d, J = 10.8 Hz, 18H). $^{13}C\{^1H\}$ NMR ($CDCl_3$, 100 MHz): δ 167.7, 152.7, 146.8, 140.8, 128.8, 125.7, 122.9, 110.1, 40.6, 35.8, 32.0, 31.2. HRMS (ESI-TOF) m/z: $[M + H]^+$ Calcd for $C_{30}H_{41}N_2$ 429.3264; Found 429.3262. Anal. Calcd for $C_{30}H_{40}N_2$: C, 84.06; H, 9.41; N, 6.54. Found: C, 83.88; H, 9.35; N, 6.76.

1-Bromo-4-*tert*-butyl-2-nitrobenzene ($\mathbf{N_2}$).[20] The compound of 4-*tert*-butylbromobenzene (18.70 g, 88.20 mmol) was carefully added to the mixture solution of concentrated sulfuric acid (10.00 mL) and nitric acid (9.00 mL). The mixture was stirred for 20 h at 30 °C. After poured into ice water, the mixture was extracted with Et_2O and washed with saturated brine. The combined organic phases were dried over $MgSO_4$ and concentrated. The residue was recrystallized in isopropanol to give N_2 (20.10 g, 89%).

4,4'-Di-*tert*-butyl-2,2'-dinitro-1,1'-biphenyl ($\mathbf{C_2}$). To a solution of $\mathbf{N_2}$ (20.00 g, 77.82 mmol) in DMF (240 mL), copper powder (10.80 g, 169.94 mmol) was added. The mixture was stirred under reflux in nitrogen atmosphere for 3 h. After the mixture was cooled to room temperature, the precipitate was filtered and DMF was evaporated

under reduced pressure. The residue was dissolved in DCM and washed with saturated brine. The combined organic phase was dried over anhydrous $MgSO_4$ and concentrated. After the residue was recrystallized in ethanol, the product was obtained as a yellow solid (12.30 g, 89%). ^{1}H NMR (400 MHz, $CDCl_3$): δ 8.18 (d, J = 1.6 Hz, 2H), 7.67 (dd, J = 8.0, 1.7 Hz, 2H), 7.21 (d, J = 8.0 Hz, 2H), 1.41 (s, 18H). ^{13}C{^{1}H} NMR (100 MHz, $CDCl_3$): δ 152.9, 147.3, 131.2, 130.8, 130.5, 121.7, 35.1, 31.1.

4,4'-Di-*tert*-butyl-[1,1'-biphenyl]-2,2'-diamine (R_2). According to the procedure for **R_1**, the reaction mixture of glacial acetic acid (100 mL), **C_2** (5.00 g, 14.04 mmol) and iron powder (11.00 g 196.43 mmol) was heated at 80 °C for an hour. After cooling to room temperature, the iron powder was removed by filtration. After a large amount of water was added to the filtrate, solid appeared in the solution. The crude product was collected by filtration and used directly in the next step without further purification. The amidation yield is the total yield of the two steps.

N,N'-(4,4'-Di-*tert*-butyl-[1,1'-biphenyl]-2,2'-diyl)diacetamide (A_2-1). Acetyl chloride (5.00 g, 63.69 mmol) was added dropwise to the mixture solution of **R_2** (3.80 g, 12.83 mmol), triethylamine (5 mL) and anhydrous CH_2Cl_2 (120 mL) at 0 °C. After stirring at room temperature overnight, the reaction solution was extracted with CH_2Cl_2 and water. The combined organic extracts were dried over anhydrous $MgSO_4$ and evaporated to dryness. The residue was purified by chromatography on silica gel column eluting with CH_2Cl_2/EA (v/v, 5/1) to afford **A_2-1** as a white solid (2.90 g, 60%). FT-IR (powder, cm^{-1}): 3403, 3306, 2950, 1667, 1557, 1524, 1460, 1412, 1366, 1273, 822, 642, 556, 510. mp 171−172 °C. ^{1}H NMR (400 MHz, $CDCl_3$): δ 8.20 (s,

2H), 7.24 (d, J = 1.8 Hz, 2H), 7.12 (d, J = 8.0 Hz, 2H), 6.93 (s, 2H), 1.99 (s, 6H), 1.38 (s, 18H). $^{13}C\{^1H\}$ NMR (100 MHz, $CDCl_3$): δ 169.2, 152.3, 135.3, 130.2, 126.5, 122.3, 120.7, 34.9, 31.3, 24.2. HRMS (ESI-TOF) m/z: $[M + Na]^+$ Calcd for $C_{24}H_{32}N_2NaO_2$ 403.2356; Found 403.2362. Anal. Calcd for $C_{24}H_{32}N_2O_2$: C, 75.75; H, 8.48; N, 7.36. Found: C, 75.49; H, 8.67; N, 7.59.

2,7-Di-*tert*-butyl-5,10-dimethylpyrido[2,3,4,5-lmn] phenanthridine (4,9-NPy-1). **A_2-1** (0.20 g, 0.53 mmol) was carefully added to the melt of aluminium chloride (0.70 g, 5.25 mmol) and sodium chloride (0.40 g, 6.84 mmol) at 100 °C in nitrogen atmosphere. After the mixture was heated to 250 °C for 8 h, ice water was added carefully. The aqueous layer was basified with sodium hydroxide, then the precipitated powder was filtered and purified by chromatography on silica gel column eluting with CH_2Cl_2 to afford **4,9-NPy-1** (0.06 g, 33%) as a light yellow solid. FT-IR (powder, cm^{-1}): 2952, 1559, 1355, 1244, 875, 653, 556. mp 294–296 °C. ^1H NMR (400 MHz, $CDCl_3$): δ 8.63 (s, 2H), 8.45 (s, 2H), 3.22 (s, 6H), 1.61 (s, 18H). $^{13}C\{^1H\}$ NMR (100 MHz, $CDCl_3$): δ 160.7, 151.7, 141.1, 126.3, 124.3, 119.3, 118.0, 35.5, 31.4, 23.3. HRMS (ESI-TOF) m/z: $[M + H]^+$ Calcd for $C_{24}H_{29}N_2$ 345.2325; Found 345.2328. Anal. Calcd for $C_{24}H_{28}N_2$: C, 83.68; H, 8.19; N, 8.13. Found: C, 83.36; H, 8.23; N, 7.77.

4,4'-Dibromo-2,2'-dinitrobenzene (C_3).[20] 2,5-Dibromonitrobenzene (5.00 g, 17.93 mmol) and copper powder (2.50 g, 39.34 mmol) were added to DMF (70 mL). The mixture was stirred at 125 °C for 3.5 h. After cooling, the precipitate was filtered and DMF was evaporated under reduced pressure. The residue was dissolved in DCM and

washed with saturated brine. The combined organic phase was dried over anhydrous $MgSO_4$ and concentrated. After the residue was recrystallized in ethanol, 4,4'-dibromo-2,2'-dinitrobenzene was obtained as a yellow solid (2.63 g, 73%).^{1}H NMR (400 MHz, $CDCl_3$): δ 8.39 (s, 2H), 7.83 (d, J = 8.2 Hz, 2H), 7.16 (d, J = 8.2 Hz, 2H). ^{13}C{^{1}H} NMR (100 MHz, $CDCl_3$): δ 147.5, 136.9, 132.2, 132.2, 128.2, 123.1.

4,4'-Dibromo-[1,1'-biphenyl]-2,2'-diamine (R_3). **R_3** was synthesized following the procedure for **R_2**, with **C_3** (1.00 g, 2.48 mmol), iron powder (1.66 g 29.64 mmol) in glacial acetic acid (70 mL) as reagents. The crude product was collected by filtration and used directly in the next step without further purification. The amidation yield is the total yield of the two steps.

N,N'-(4,4'-Dibromo-[1,1'-biphenyl]-2,2'-diyl)diacetamide (**A_3**). **A_3** was synthesized following the procedure for **A_2-1**, with **R_3** (1.00 g), Et_3N (1.00 mL), acetyl chloride (1.14 g, 14.52 mmol) in CH_2Cl_2 (60 mL) as reagents. The desired product **A_3** was obtained as an off-white solid (0.61 g, 57%). FT-IR (powder, cm^{-1}): 3405, 3281, 1675, 1504, 1402, 1270, 1006, 869, 811, 588. mp 145–146 ^{o}C. ^{1}H NMR (400 MHz, $CDCl_3$): δ 8.33 (s, 2H), 7.39 (d, J = 8.1 Hz, 2H), 7.04 (d, J = 8.1 Hz, 2H), 6.84 (s, 2H), 2.00 (s, 6H). ^{13}C{^{1}H} NMR (100 MHz, $CDCl_3$): δ 169.1, 136.5, 131.6, 128.5, 126.9, 126.5, 123.4, 24.2. HRMS (ESI-TOF) m/z: $[M + Na]^+$ Calcd for $C_{16}H_{14}Br_2N_2NaO_2$ 448.9295; Found 448.9296. Anal. Calcd for $C_{16}H_{14}Br_2N_2O_2$: C, 45.10; H, 3.31; N, 6.57; O, 7.51. Found: C, 45.08; H, 3.56; N, 6.44; O, 7.66.

2,7-Dibromo-5,10-dimethylpyrido[2,3,4,5-lmn]phenanthridine (4,9-NPy-Br). **4,9-NPy-Br** was synthesized following the procedure for **4,9-NPy-1**, with **A_3** (0.5 g,

1.18 mmol), aluminium chloride (1.40 g, 10.50 mmol) and sodium chloride (0.90 g, 15.40 mmol) as reagents. The desired product **4,9-NPy-Br** was obtained as a light yellow solid (0.18 g, 39%). FT-IR (powder, cm^{-1}): 1554, 1426, 1326, 1023, 865, 815, 673, 558. mp > 300 °C. ^1H NMR (400 MHz, $CDCl_3$): δ 8.69 (s, 2H), 8.56 (s, 2H), 3.18 (s, 6H). This compound is too insoluble to record a $^{13}C\{^1H\}$ NMR spectrum. HRMS (ESI-TOF) m/z: $[M + H]^+$ Calcd for $C_{16}H_{11}Br_2N_2$ 390.9264; Found 390.9258. Anal. Calcd for $C_{16}H_{10}Br_2N_2$: C, 49.27; H, 2.58; N, 7.18. Found: C, 49.17; H, 2.48; N, 7.21.

2,7-Di-*tert*-butylpyrene (Py-tBu).[12] **Py-tBu** was synthesized according to the reported procedure. ^1H NMR (400 MHz, $CDCl_3$): δ 8.18 (s, 2H), 8.02 (s, 2H), 1.56 (s, 18H).

2,7-Bis(9,9-dioctyl-9H-fluoren-2-yl)-5,10-dimethylpyrido[2,3,4,5-lmn]phenanthridine (Fl-NPy). A mixture of **4,9-NPy-Br** (300 mg, 0.8 mmol), 9,9-dioctyl-2-boronic ester-fluorene (1.00 g, 1.94 mmol), $NaHCO_3$ (1.30 g, 15.47 mmol), THF (50 mL) and H_2O (20 mL) was degassed before and after $Pd(PPh_3)_4$ (18 mg, 0.015 mmol) was added. The mixture was heated to reflux and stirred under nitrogen for 24 h. The reaction mixture was extracted with CH_2Cl_2 (3 × 100 mL), and the combined organic layers were dried over anhydrous $MgSO_4$ and concentrated under reduced pressure. The residue was purified by chromatography on silica gel column eluting with petroleum ether/CH_2Cl_2 (v:v, 2:3) to afford **Fl-NPy** as an ivory solid (0.57 g, 74%). FT-IR (powder, cm^{-1}): 2920, 2843, 1441, 1361, 868, 829, 736. mp > 300 °C. ^1H NMR (400 MHz, $CDCl_3$) δ 8.90 (s, 2H), 8.74 (s, 2H), 7.91 (s, 4H), 7.89 (s, 2H), 7.80 (d, J = 7.0 Hz, 2H), 7.37 (dd, J = 15.0, 7.8 Hz, 6H), 3.34 (s, 6H), 2.12–2.01 (m, 8H), 1.55 (s,

10H), 1.20–1.00 (m, 38H), 0.78 (t, J = 6.9 Hz, 12H). $^{13}C\{^{1}H\}$ NMR (100 MHz, $CDCl_3$) δ 161.3, 152.0, 151.1, 142.3, 141.2, 140.5, 127.9, 127.4, 126.9, 126.9, 126.1, 125.2, 123.0, 122.6, 122.2, 121.3, 120.4, 120.0, 119.3, 55.4, 40.5, 31.8, 29.3, 29.2, 23.9, 23.5, 22.6, 14.0. HRMS (ESI-TOF) m/z: $[M + H]^+$ Calcd for $C_{74}H_{93}N_2$ 1009.7333; Found 1009.7339. Anal. Calcd for $C_{74}H_{92}N_2$: C, 88.04; H, 9.19; N, 2.77. Found: C, 87.06; H, 8.87; N, 2.63.

Acknowledgements

This work was supported by the National Key Research and Development Program of China (Grants 2017YFA0204503 and 2017YFA0207800), the National Natural Science Foundation of China (Grants 21522405, 51503142 and 21734006) is gratefully acknowledged. We thank Dr. X. W. Lou (Eindhoven University of Technology) for helpful discussions about the manuscript.

Supporting Information

^{1}H NMR and $^{13}C\{^{1}H\}$ NMR spectra and HRMS (ESI-TOF) spectra, single crystal data, UV-vis absorption spectra, fluorescence spectra, photographs, TGA data, computational data. The Supporting Information is available free of charge on the ACS Publications website at DOI: xxx

Author Information

Corresponding Author

*E-mail:yulan.chen@tju.edu.cn; lmw@tju.edu.cn

Author Contributions

§Yi Han and Zhenzhu Hu contributed equally to this work.

Notes and References

1. (a) Watanabe, M.; Chang, Y. J.; Liu, S.-W.; Chao, T.-H.; Goto, K.; Islam, M. M.; Yuan, C.-H.; Tao, Y.-T.; Shinmyozu, T.; Chow, T. J. The Synthesis, Crystal Structure and Charge-Transport Properties of Hexacene. *Nat. Chem.* **2012**, *4*, 574. (b) Segawa, Y.; Maekawa, T.; Itami, K. Synthesis of Extended π-Systems through C–H Activation. *Angew. Chem., Int. Ed.* **2015**, *54*, 66.

2. (a) Anthony, J. E. Functionalized Acenes and Heteroacenes for Organic Electronics. *Chem. Rev.* **2006**, *106*, 5028. (b) Bunz, U. H. F. The Larger Linear N-Heteroacenes. *Acc. Chem. Res.* **2015**, *48*, 1676. (c) Chen, Y.; Marszalek, T.; Fritz, T.; Baumgarten, M.; Wagner, M.; Pisula, W.; Chen, L.; Müllen, K. Contorted Polycyclic Aromatic Hydrocarbons with Cove Regions and Zig-Zag Edges. *Chem. Commun.* **2017,** *53*, 8474. (d) Murai, M.; Iba, S.; Ota, H.; Takai, K. Azulene-Fused Linear Polycyclic Aromatic Hydrocarbons with Small Bandgap, High Stability, and Reversible Stimuli Responsiveness. *Org. Lett*. **2017**, *19*, 5585.

3. (a) Li, J.; Chen, S.; Wang, Z.; Zhang, Q. Pyrene-fused Acenes and Azaacenes: Synthesis and Applications. *Chem. Rec.* **2016**, *16*, 1518. (b) Chen, W.; Li, X.; Long, G.; Li, Y.; Ganguly, R.; Zhang, M.; Aratani, N.; Yamada, H.; Liu, M.; Zhang, Q. Pyrene-Containing Twistarene: Twelve Benzene Rings Fused in a Row

Angew. Chem., Int. Ed. **2018**, *57*, 13555. (c) Gu, P.; Wang, Z.; Liu, G.; Yao, H.; Wang, Z.; Li, Y.; Zhu, J.; Li, S.; Zhan, Q. Synthesis, Full Characterization, and Field Effect Transistor Behavior of a Stable Pyrene-Fused N-Heteroacene with Twelve Linearly Annulated Six-Membered Rings. *Chem. Mater.* **2017**, *29*, 4172. (d) Wang, Z.; Gu, P.; Liu, G.; Yao, H.; Wu, Y.; Li, Y.; Rakesh, G.; Zhu, J.; Fu, H.; Zhang, Q. A Large Pyrene-Fused N-Heteroacene: Fifteen Aromatic Six-Membered Rings Annulated In One Row. *Chem Commun.* **2017**, *53*, 7772.

4. (a) Mosca, L.; Karimi Behzad, S.; Anzenbacher, P. Small-Molecule Turn-On Fluorescent Probes for RDX. *J. Am. Chem. Soc.* **2015,** *137*, 7967. (b) Liu, P.; Sun, S.; Guo, X.; Yang, X.; Huang, J.; Wang, K.; Wang, Q.; Liu, J.; He, L. Competitive Host–Guest Interaction between β-Cyclodextrin Polymer and Pyrene-Labeled Probes for Fluorescence Analyses. *Anal. Chem.*, ***2015***, *87*, 2665. (c) Zou, L.; Wang, X.-Y.; Zhang, X.-X.; Dai, Y.-Z.; Wu, Y.-D.; Wang, J.-Y.; Pei, J. Toward Electron-Deficient Pyrene Derivatives: Construction of Pyrene Tetracarboxylic Diimide Containing Five-Membered Imide Rings. *Chem. Commun.* **2015**, *51*, 12585. (d) Min, Y.; Dou, C.; Tian, H.; Geng, Y.; Liu, J.; Wang, L. n-Type Azaacenes Containing B←N Units**.** *Angew. Chem., Int. Ed.* **2018**, *57*, 2000. (e) Taher, A.; Lee, K. C.; Han, H. J.; Kim, D. W. Pyrene-Tagged Ionic Liquids: Separable Organic Catalysts for S_N2 Fluorination. *Org. Lett.* **2017**, *19*, 3342.

5. (a) Chen, M.; Chen, R.; Shi, Y.; Wang, J.; Cheng, Y.; Li, Y.; Gao, X.; Yan, Y.; Sun, J. Z.; Qin, A.; Kwok, R. T. K.; Lam, J. W. Y.; Tang, B. Z.

Malonitrile-Functionalized Tetraphenylpyrazine: Aggregation-Induced Emission, Ratiometric Detection of Hydrogen Sulfide, and Mechanochromism. *Adv. Funct. Mater*., **2018**, *28*, 1704689. (b) Ito, S.; Tokimaru, Y.; Nozaki, K. Benzene-Fused Azacorannulene Bearing an Internal Nitrogen Atom. *Angew. Chem., Int. Ed.* **2015**, *54*, 7256. (c) Tan, Y.-Z.; Osella, S.; Liu, Y.; Yang, B.; Beljonne, D.; Feng, X.; Müllen, K. Sulfur-Annulated Hexa-*peri*-hexabenzocoronene Decorated with Phenylthio Groups at the Periphery. *Angew. Chem., Int. Ed.* **2015**, *54*, 2927.

6. (a) Kiel, G. R.; Samkian, A. E.; Nicolay, A.; Witzke, R. J.; Tilley, T. D. Titanocene-Mediated Dinitrile Coupling: A Divergent Route to Nitrogen-Containing Polycyclic Aromatic Hydrocarbons. *J. Am. Chem. Soc.* **2018**, *140*, 2450. (b) Xie, G.; Hahn, S.; Rominger, F.; Freudenberg, J.; Bunz, U. H. F. Synthesis and Characterization of Two Different Azarubrenes**.** *Chem. Commun.* **2018**, *54*, 7593. (c) Tan, Q.; Higashibayashi, S.; Karanjit, S.; Sakurai, H. Enantioselective Synthesis of a Chiral Nitrogen-Doped Buckybowl. *Nat. Commun.* **2012**, *3*, 891. (d) Skabeev, A.; Zschieschang, U.; Zagranyarski, Y.; Klauk, H.; Müllen, K.; Li, C. Carbonyl-Functionalized Cyclazines as Colorants and Air-Stable *n*-Type Semiconductors**.** *Org. Lett.* **2018**, *20*, 1409-1412.
7. Nakazato, T.; Kamatsuka, T.; Inoue, J.; Sakurai, T.; Seki, S.; Shinokubo, H.; Miyake, Y. The Reductive Aromatization of Naphthalene Diimide: A Versatile Platform for 2, 7-Diazapyrenes. *Chem. Commun.* **2018**, *54*, 5177.
8. Robbins, R. F. Some Derivatives of 4, 9-Diazapyrene. *J. Chem. Soc.,* **1960**, 2553.
9. (a) Coffin, B.; Robbins, R. F. *J.* 4,10-Diaxapyrenes. *Chem. Soc.,* **1965**, 3379. (b)

Tanga, M. J.; Reist, E. J**.** Synthesis of 1-azapyrene. *J. Heterocycl. Chem.* **1986**, *23*, 747.

10. (a) Wang, T.; Wang, H.; Li, G.; Li, M.; Bo, Z.; Chen, Y. Thiophene-Fused 1,10-Phenanthroline and Its Conjugated Polymers. *Macromolecules* **2016**, *49*, 4088. (b) Guo, H.; Liu, M.; Han, Y.; Han, S.; Chen, Y. Synthesis and Characterization of *S, N*-Heteroacenes by Bischler-Napieralski Reaction. *Chin. J. Polym. Sci.* **2016**, *34*, 1319. (c) Yuan, W.; Ren, X.-K.; Li, M.; Guo, H.; Han, Y.; Wu, M.; Wang, Q.; Li, M.; Chen, Y. From S,N-Heteroacene to Large Discotic Polycyclic Aromatic Hydrocarbons (PAHs): Liquid Crystal versus Plastic Crystalline Materials with Tunable Mechanochromic Fluorescence. *Angew. Chem., Int. Ed.* **2018**, *57*, 6161.
11. Tan, Q.; Chen, H.; Xia, H.; Liu, B.; Xu, B. Parent and Trisubstituted Triazacoronenes: Synthesis, Crystal Structure and Physicochemical Properties. *Chem. Commun.* **2016**, *52*, 537.
12. Gu, P.-Y.; Zhang, J.; Long, G.; Wang, Z.; Zhang, Q. Solution-Processable Thiadiazoloquinoxaline-Based Donor-Acceptor Small Molecules for Thin-Film Transistors**.** *J. Mater. Chem. C* **2016**, *4*, 3809.
13. Li, Q.; Zhang, S.; Dai, L.; Li, L. Nitrogen-Doped Colloidal Graphene Quantum Dots and Their Size-Dependent Electrocatalytic Activity for the Oxygen Reduction Reaction. *J. Am. Chem. Soc.* **2012**, *134*, 18932.
14. Bañuelos Prieto, J.; López Arbeloa, F.; Martínez Martínez, V.; Arbeloa López, T.; López Arbeloa, I. Photophysical Properties of the Pyrromethene 597 Dye:

Solvent Effect. *J. Phys. Chem. A* **2004**, *108*, 5503.

15. Wang, X.-Y.; Lin, H.-R.; Lei, T.; Yang, D.-C.; Zhuang, F.-D.; Wang, J.-Y.; Yuan, S.-C.; Pei, J. Azaborine Compounds for Organic Field-Effect Transistors: Efficient Synthesis, Remarkable Stability, and BN Dipole Interactions. *Angew. Chem., Int. Ed.* **2013**, *52*, 3117.
16. (a) He, B.; Dai, J.; Zherebetskyy, D.; Chen, T. L.; Zhang, B. A.; Teat, S. J.; Zhang, Q.; Wang, L.; Liu, Y. A Divergent Route to Core-and Peripherally Functionalized Diazacoronenes that Act as Colorimetric and Fluorescence Proton Sensors. *Chem. Sci.* **2015**, *6*, 3180. (b) Park, Y. S.; Dibble, D. J.; Kim, J.; Lopez, R. C.; Vargas, E.; Gorodetsky, A. A. Synthesis of Nitrogen-Containing Rubicene and Tetrabenzopentacene Derivatives. *Angew. Chem., Int. Ed.* **2016**, *55*, 3352.
17. (a) Li, M.; Yuan, Y.; Chen, Y. Acid-Induced Multicolor Fluorescence of Pyridazine Derivative. *ACS Appl. Mater. Interfaces* **2018**, *10*, 1237. (b) Tang, R.; Wang, X.; Zhang, W.; Zhuang, X.; Bi, S.; Zhang, W.; Zhang, F. Aromatic Azaheterocycle-Cored Luminogens with Tunable Physical Properties *via* Nitrogen Atoms for Sensing Strong Acids. *J. Mater. Chem. C* **2016**, *4*, 7640.
18. Tolman, C. A.; Seidel, W. C.; Gerlach, D. H. Triarylphosphine and Ethylene Complexes of Zerovalent Nickel, Palladium, and Platinum. *J. Am. Chem. Soc.* **1972**, *94*, 2669.
19. Ashton, P. R.; Harris, K. D. M.; Kariuki, B. M.; Philp, D.; Robinson J. M. A.; Spencer, N. A Borazaaromatic Analogue of Isophthalic Acid. *J. Chem. Soc.* **2001**,

2, 2166.

20. Wegner, H. A.; Reisch, H.; Rauch, K.; Demeter, A.; Zachariasse, K. A.; Meijere, A.; Scott, L. T. Oligoindenopyrenes: A New Class of Polycyclic Aromatics. *J. Org. Chem.* **2006**, *71*, 9080.